

doi:10.15199/48.2020.11.18

Millimeter-Wave switched beam antenna with parasitic ring for 5G applications

Abstract. This paper proposes the switched beam antenna with a parasitic ring on single patch which operate at 5G frequency. 28.5 GHz frequency band which is one band of millimeter-wave for 5G applications is used to design the antenna. Beam direction can be switched by shorted circuit at patch and parasitic. There are 4 cases of beam switching with maximum gain of 8.06 dBi. In this paper, the single element switched beam antenna which high gain, low profile and small in size is achieved.

Streszczenie. Przedstawiono antenę z przełączanym strumieniem pracującą przy częstotliwości 28,5 GHz co umożliwia pracę w zakresie fal milimetrowych systemu 5G. Możliwe jest przełączanie między czterema strumieniami ze wzmocnieniem 8.06 dBi. (Przełączalna antena w paśmie milimetrowym do zastosowań 5G)

Keywords: mm wave, switched beam, 5G, parasitic

Słowa kluczowe: zakres fal milimetrowych, antena, system 5G

Introduction

5th generation (5G) of wireless communications technologies [1] are improved to manage the problems due to the tremendous increasing of demand in wireless communications. The high-frequency bands which are referred to as millimeter wavelength (mm wave) from 24 GHz up to 100 GHz are proposed to support wide bandwidth and high data rate in 5G technologies. However, to use high-frequency bands the high propagation losses and blocking are occurred. One technique that capable to cope these problems is utilizing smart antenna systems. Smart antenna system [2] are composed with 2 major parts that are antenna array and signal processing system. Main beam direction can point to desired signal while null can steer to interference directions using smart antenna. Switched beam antenna or fixed beam antenna is one category of smart antenna that has low profile and low complex processing. This system consists of antenna array and beamforming network. Fixed beams are steered to multiple directions and signal strength of each direction is detected. Thereafter, the beam direction that provide the highest signal strength is chosen when position of user is fixed during the beam direction is switched when position of user is moved.

Low profile structure and small in size of switched beam antenna has interested to use at mobile terminal. Several researchers present a low complex switched beam antenna using single element such as the paper presented in [3] the beam switching using a spiral antenna which radiation pattern can be switched by adjusting the length of spiral. A square loop antenna in [4] which main beam direction can be steered by changing positions of feeding points. However, these antennas are not considerably suitable for dynamic system. Also, a fixed-size and fixed-feeding point of rectangular patch in [5], octagonal patch in [6] and [7] that can operate at 2.45 GHz which beam direction can be changed by short circuit at terminal edges have revealed. Moreover, considerable literatures reveal low complex antenna for 5G technology such as triangular-shaped slot antenna array which operated frequencies are 28 GHz and 38 GHz for 5G applications in [8]. In this work, bandwidth of the antenna can increase by etching triangular-shaped slot on the ground plane. Moreover, the antenna gain can be increased by addition of radiating elements. The 28 GHz and 38 GHz MIMO antennas for 5G mobile applications were presented in [9]. There are anticipated results which are appropriate for next 5G communication applications. The four element MIMO antenna provides the maximum

gain of 7.95 dBi at 28 GHz while the two element symmetric antenna provides the maximum gain of 9.49 dBi at 38 GHz. Moreover, the design of 28/38 GHz for 5G mobile communication networks was presented in [10] which the antenna provides omni directional patterns, flat gain of 7 dBi and high radiation efficiency. A multiband antenna for 5G technologies which has low cost and good radiation control was presented in [11]. This antenna can operate multi frequencies using only single element. Gain of antenna in 5G frequency, 26 GHz, is 2.4 dBi. The design of antenna array for 5G mm-wave system was proposed in [12] which is four typical planar antenna array architectures are discussed. However, main beam direction of the antennas presented in [8] – [12] cannot switch. As mentioned above, more advancements of the antenna for 5G communication have been accomplished when cooperate with switched beam antenna. Therefore, this article proposes the design of low profile switched beam antenna for 5G communications. The antenna operates at 28.5 GHz which is 5G mm wave spectrum. The single element of octagonal patch is designed to provide 4 different directions with the maximum gain is 8.06 dBi while a parasitic ring is designed to reduce sidelobe level. The width, height and length of the proposed antenna is 14.948x0.288x14.948 mm³. Therefore, a low profile and small in size antenna is achieved.

The rest of this article is as follows. After brief introduction, the design of antenna is described in Antenna configuration section. Next, sidelobe reduction using parasitic element and beam switching by short circuit are revealed in Simulation and results section. The performance in term of SIR is considered in The performance of the systems section. Finally, Conclusion section is concluded the paper.

Antenna configuration

The proposed antenna has been designed on RT5880 with dielectric constant (ϵ_r) of 2.2 substrate thickness (h) of 0.254 mm and resonant frequency of 28 GHz. The antenna consists with the octagonal patch with thickness (t) of 0.017 mm on the center of the square substrate and 0.017 mm height (G) of ground plane. The octagonal patch is designed based on circular shape then divided into 8 sections. Radius of circular shape is used to be radius of octagonal patch which can be given by [13].

$$(1) \quad r = \frac{F}{\left\{ 1 + \frac{2h}{\pi \epsilon_r F} \left[\ln \left(\frac{\pi F}{2h} \right) + 1.7726 \right] \right\}^2}$$

where

$$(2) \quad F = \frac{8.79 \times 10^9}{f_r \sqrt{\epsilon_r}}$$

Next, the octagonal shape is calculated from the radius r by

$$(3) \quad \frac{Y}{r} = \cos 67.5^\circ$$

$$(4) \quad \frac{X}{r} = \sin 67.5^\circ$$

where X and Y are shown in Fig.1. Thereafter, S_{11} is simulated when feeding point is at center of the antenna. However, the antenna cannot operate at 28 GHz. Therefore, the radius of octagonal patch is adjusted by 0.1 mm increasing in each step while size of substrate and ground plane are based on $\lambda \times \lambda$ then adjusted by 0.1λ increasing in each step which changing of S_{11} result is shown in Fig.2. From the result, the antenna can operate at 28 GHz when the radius of patch is 4.474 mm and dimension of substrate and ground plane are $14.948 \times 14.948 \text{ mm}^2$ as shown in Fig.3.

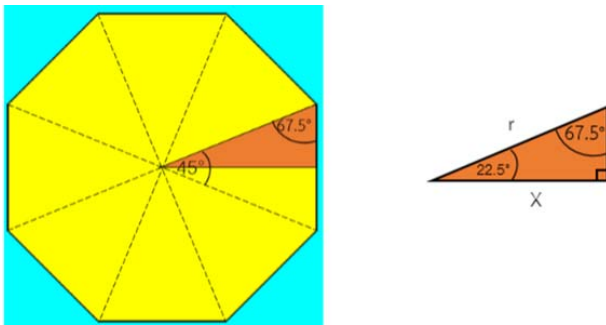


Fig.1. Structure of octagonal patch.

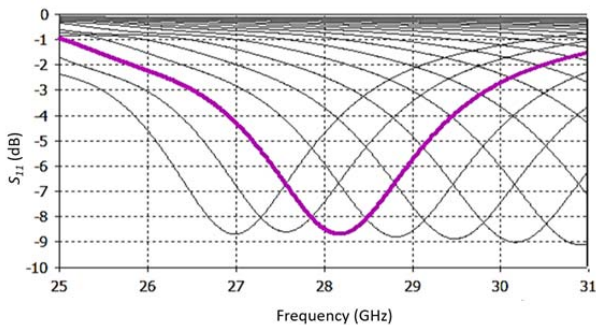


Fig.2. S_{11} of the octagonal with radius r .

Afterwards, main beam directions are switched by shorted-circuit at the corner of octagonal patch. The choice of shorted-circuit position is due to the current distribution on the patch. The antenna has maximum distribution at the patch center while low current distribution occurs at the patch corners. There are 4 cases of shorted circuit positions which are shown in Fig.4 to Fig.7 as are called case 1 to case 4. In case 1, main beam directions are $122^\circ/300^\circ$ when shorted-circuit positions are $112.5^\circ/292.5^\circ$ as shown in Fig.4. Main beam directions are $148^\circ/330^\circ$ when shorted-circuit positions are $157.5^\circ/337.5^\circ$ which is called case 2 as shown in Fig.5. Main beam directions are $30^\circ/212^\circ$ when shorted-circuit positions are $22.5^\circ/202.5^\circ$ in case 3 as

shown in Fig.6. In case 4, main beam directions are $58^\circ/240^\circ$ when shorted-circuit positions are $67.5^\circ/247.5^\circ$ as shown in Fig.7. As we can see, directions of main beam have the same trend with positions of shorted circuit. This is due to positions of shorted circuit is act as director.

However, there are high level of side lobe in 4 cases. Therefore, parasitic ring is combined on patch to reduce side lobe level of the antenna as is discuss in next section.

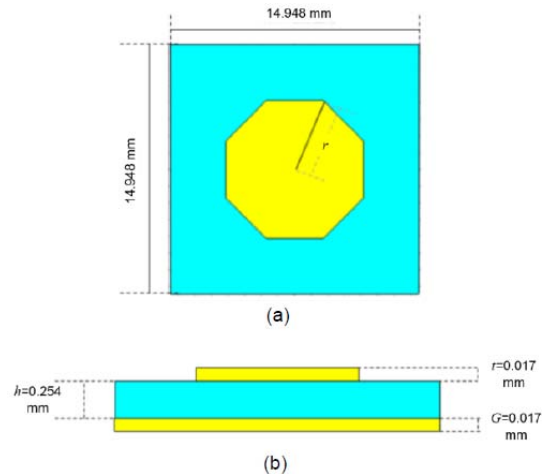


Fig.3. The antenna structure (a) top view (b) side view.

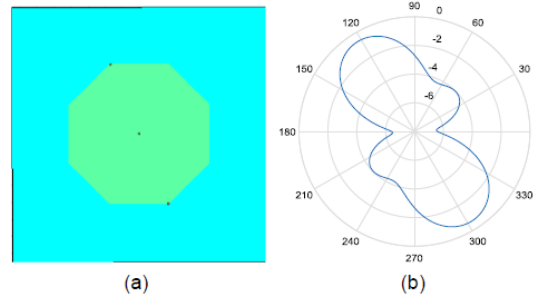


Fig.4. (a) Positions of shorted-circuit and (b) radiation pattern of case 1.

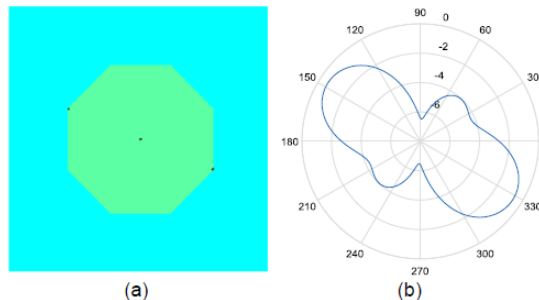


Fig.5. (a) Positions of shorted-circuit and (b) radiation pattern of case 2.

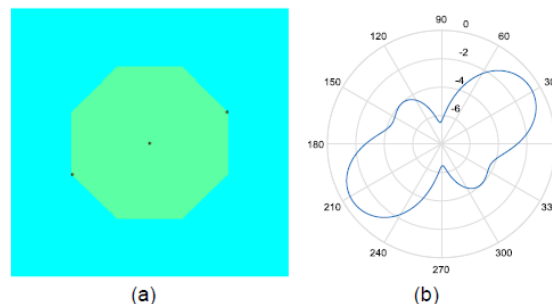


Fig.6. (a) Positions of shorted-circuit and (b) radiation pattern of case 3.

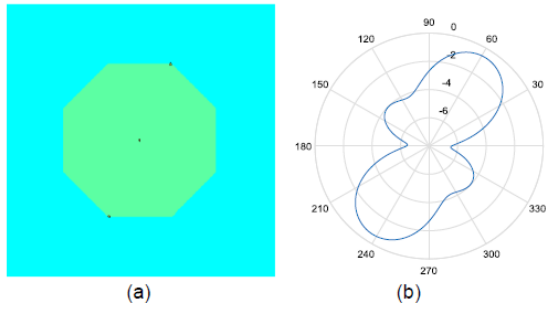


Fig.7. (a) Positions of shorted-circuit and (b) radiation pattern of case 4.

Simulation and results

In this section parasitic ring is adopted to reduce side lobe level of the antenna. A ring with outer radius of 6.174 mm and inner radius of 4.574 mm is combined with octagonal patch. At first, 112.5° and 292.5° of parasitic ring are shorted and different radius of shorted circuit positions are discussed. There are 4 different radius of shorted circuit positions, 4.674 mm, 5.174 mm, 5.674 mm and 5.974 mm which radiation pattern is shown in Fig. 8. As a result, there is the lowest side lobe level when the position of shorted circuit radius is 5.674 mm. Moreover, to decrease side lobe level the corner of octagonal patch is shorted while a ring is shorted at 5.674 mm as shown in Fig. 9 (a). Side lobe level can decrease when a patch and a ring are shorted as shown in Fig. 9 (b). S_{11} of the antenna when a patch and a ring are shorted are shown in Fig.10. Next, feeding point is adjusted to improve impedance matching which is calculated by [14].

$$(5) \quad X_{point} = \frac{L_p}{2\sqrt{\epsilon_{eff}}}$$

$$(6) \quad Y_{point} = \frac{W_p}{3\sqrt{\epsilon_{eff}}}$$

where X_{point} and Y_{point} are feeding point on x-y axis and L_p , W_p and ϵ_{eff} are discussed by

$$(7) \quad W_p = \frac{c}{2f_r} \left(\frac{\epsilon_r + 1}{2} \right)$$

$$(8) \quad L_p = L_{eff} - 2\Delta L$$

$$(9) \quad \epsilon_{eff} = \frac{\epsilon_r + 1}{2} + \frac{\epsilon_r - 1}{2} \left(1 + \frac{12h}{W_p} \right)^{-\frac{1}{2}}$$

where

$$(10) \quad L_{eff} = \frac{c}{2f_r \sqrt{\epsilon_{eff}}}$$

$$(11) \quad \Delta L = 0.412h \left(\frac{\epsilon_{eff} + 0.3}{\epsilon_{eff} - 0.258} \right) \left(\frac{\frac{W_p}{h} + 0.264}{\frac{W_p}{h} + 0.8} \right)$$

where ϵ_r is dielectric constant of substrate, h is the height of substrate, f_r is resonant frequency and c is phase velocity.

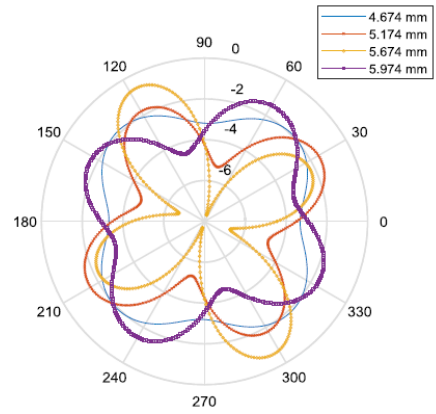


Fig.8. Radiation patterns of the antenna with different shorted circuit positions.

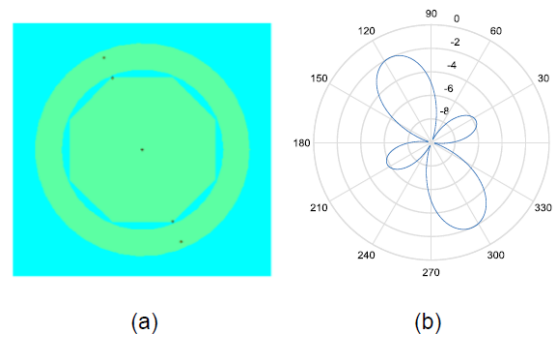


Fig.9. (a) Configuration and (b) radiation pattern when a patch and a ring are shorted.

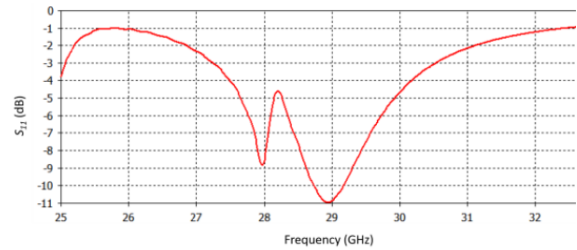


Fig.10. S_{11} of the antenna when a patch and a ring are shorted.

After feeding point is calculated, outer and inner radius of parasitic ring are adjusted to switch main beam direction. S_{11} of the antenna when feeding point is (1.12,0.983) in millimetres, outer radius of a ring is 6.094 mm and inner radius is 5.574 mm is shown in Fig. 11. As we can see, the antenna can operate at 28.5 GHz. Afterward, feeding point, outer and inner radius of parasitic are adjusted to reduce S_{11} and side lobe level. The feeding point that provide lowest S_{11} and side lobe level is (1.146,0.93) which outer and inner radius of parasitic are 6.094 mm and 4.564 mm, respectively. Thereafter, radiation patterns and S_{11} of the antenna are revealed. There are 4 cases of switching, case 1 to case 4. Case 1, the antenna is shorted at 112.5°/292.5°. Case 2, the antenna is shorted at 157.5°/337.5°. Case 3, the antenna is shorted at 22.5°/202.5° while the antenna is shorted at 67.5°/247.5° is called case 4. The antenna configurations of 4 cases are shown in Fig. 12. Next, radiation pattern of 4 cases is shown in Fig. 13 and S_{11} are shown in Fig. 14 to Fig. 17 for case 1 to case 4, respectively. Next, radiation patterns of the proposed antenna are compared with the ones without parasitic ring as shown in Fig. 18 to Fig. 21. The results of the proposed antenna with and without parasitic ring are

exposed in Table 1. As we can see that the proposed antenna, the single octagonal patch with a parasitic ring, can reduce side lobe level. Gain of antenna can be increased when parasitic ring is employed. The maximum gain is 8.06 dBi and the approximately bandwidth is 500 MHz. As a result, better gain is accomplished than some of the switched beam antenna cited works as in [3, 4, 5, 6, 7] and 5G antenna cited works as in [8, 10, 11]. Also, gain of the proposed antenna is comparable to the work presented in [9] which is four elements MIMO antenna while there is single element of the proposed antenna.

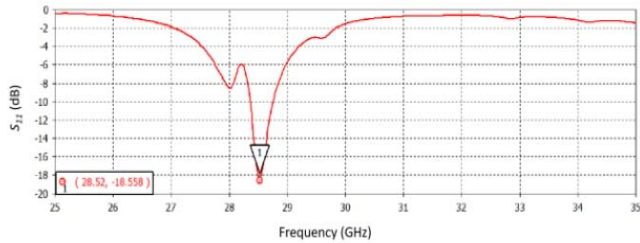


Fig.11. S_{11} of the antenna when feeding point is (1.12,0.983).

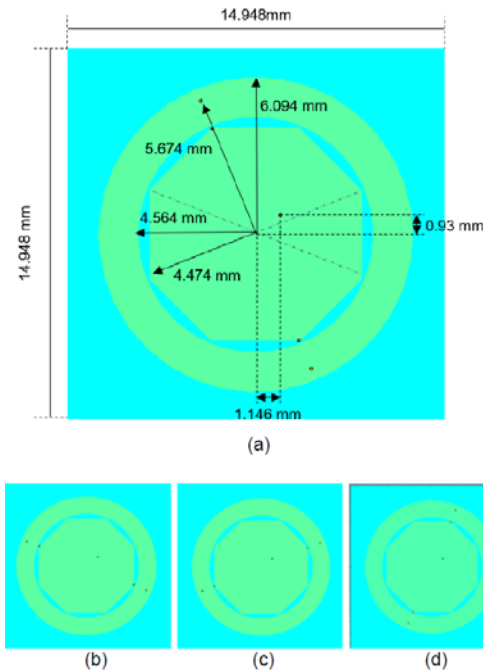


Fig.12. Configurations of the antenna when feeding point is (1.146,0.93), outer and inner radius of parasitic are 6.094 mm and 4.564 mm (a) case 1 (b) case 2 (c) case 3 (d) case 4.

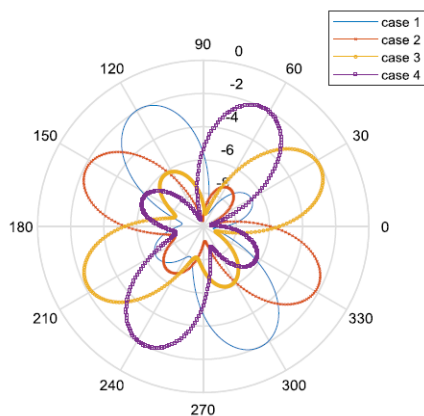


Fig.13. Radiation patterns of case 1 to case 4.

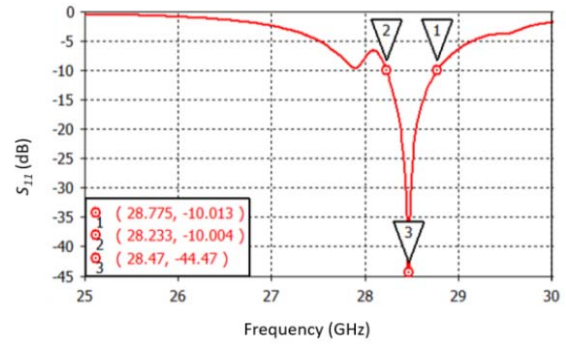


Fig.14. S_{11} of the antenna for case 1.

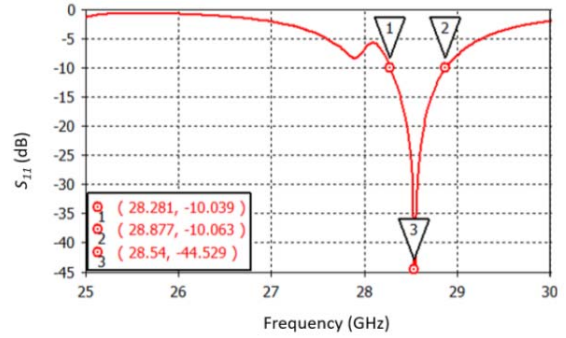


Fig.15. S_{11} of the antenna for case 2.

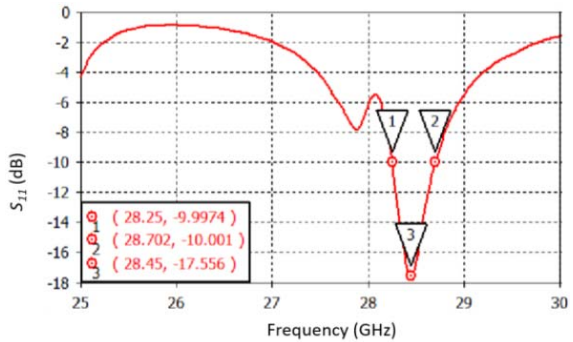


Fig.16. S_{11} of the antenna for case 3.

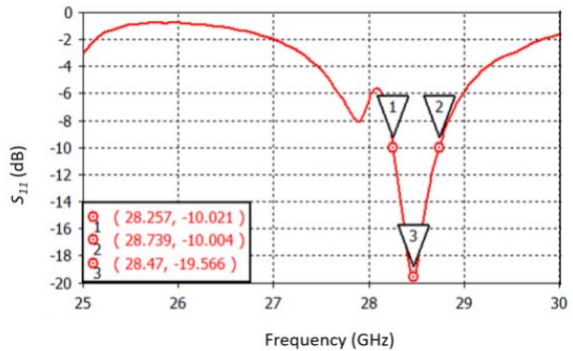


Fig.17. S_{11} of the antenna for case 4.

Table 1. The results of the proposed antenna with and without parasitic ring

Case	S_{11} (dB)	Bandwidth (MHz)	Gain (dBi)	Side lobe level (dB)	Main beam directions (degree)
Without parasitic ring					
1	-9.35	-	7.4	-3.4	122, 300
2	-9.35	-	7.4	-3.4	148, 330
3	-9.35	-	7.4	-3.4	30, 212
4	-9.35	-	7.4	-3.4	58, 240
With parasitic ring					
1	-44.47	542	8.06	-4.7	119, 299
2	-44.53	596	7.86	-4.5	154, 334
3	-17.57	452	7.92	-4.5	27, 207
4	-19.57	482	8.02	-4.0	63, 243

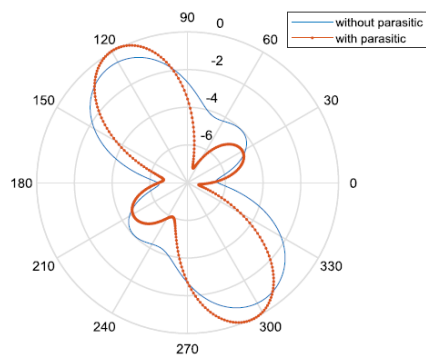


Fig.18. Radiation patterns with and without parasitic ring of case 1.

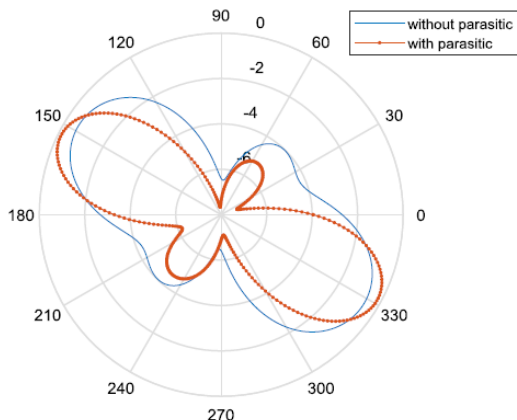


Fig.19. Radiation patterns with and without parasitic ring of case 2.

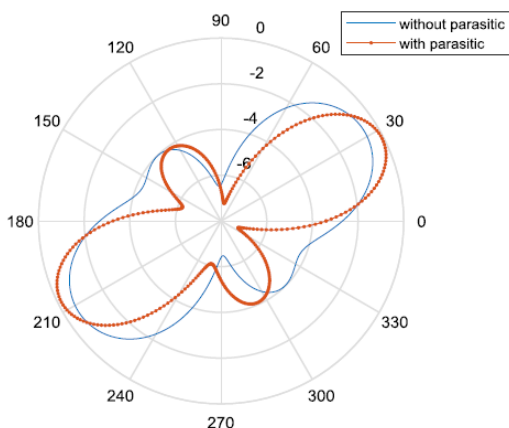


Fig.20. Radiation patterns with and without parasitic ring of case 3.

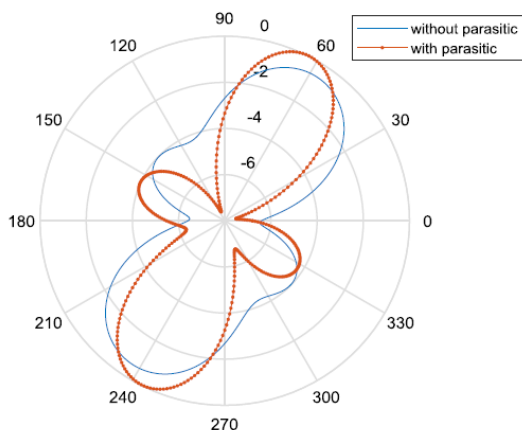


Fig.21. Radiation patterns with and without parasitic ring of case 4.

The performance of the systems

In this section, interference signals from other base stations are considered as shown in Fig. 22 which the directions of interference signals are random. The signals from neighbouring base station becomes an interferer to the user of adjacent cell as shown in Fig. 22 (a). This is due to the omni-directional beam pattern radiated from the user. To handle this problem, the beamforming technique when the beam patterns are steerable in horizontal plane is presented as shown in Fig.22 (b). Hence, it cannot only enhance the desired signal but also reduces interference transmitted from neighbouring base station. The wireless channel between the base station and the user is assumed to have effect from propagation path loss which can be given by

$$(12) \quad PL = 20 \log_{10} \left(\frac{4\pi d}{\lambda} \right)$$

where d is the distance between the user and the base station. As the received Signal-to-Interference Ratio (SIR) at i^{th} user can be obtained by [15, 16]

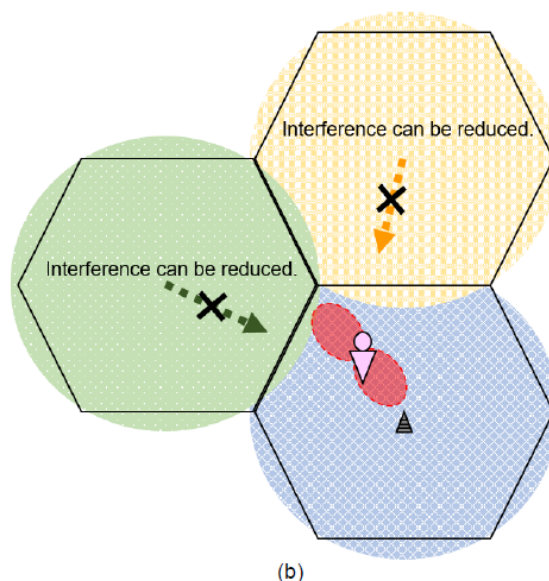
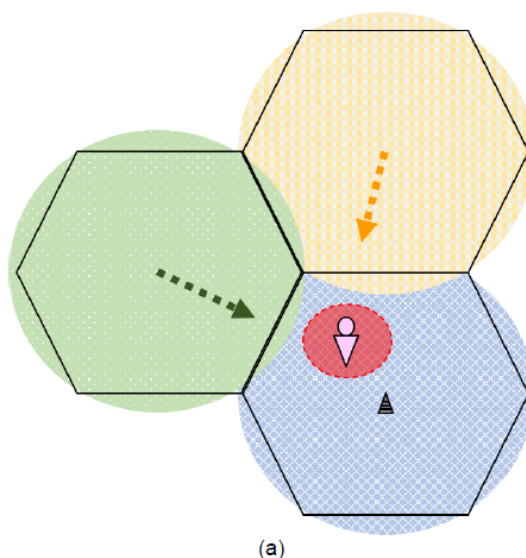


Fig.22. Interference signals from other base stations when (a) omni-directional antenna and (b) the proposed antenna are applied.

$$(13) \quad SIR_i = \frac{P_i g_i \left(10^{\frac{PL_i}{10}} \right)}{\sum_j P_j g_{i,j} \left(10^{\frac{PL_j}{10}} \right)}$$

where the P_i and P_j are the transmitted power servings at the i^{th} cell and interfering j^{th} cell, respectively. The g_i is the gain of the antenna when the i^{th} user received the signal from the i^{th} cell. In addition, $g_{i,j}$ is the gain observed between the i^{th} user and the j^{th} cell site. The PL_i and PL_j are propagation path losses from the i^{th} cell site and the j^{th} cell site to the i^{th} user, respectively.

The comparison of performance in term of SIR between three concepts is revealed in Fig. 23. The conventional concept, in which an omni-directional antenna is used, the concepts which the antenna with and without parasitic ring are utilized are discussed. It can confirm that the SIR can be clearly enhanced when apply the proposed concept.

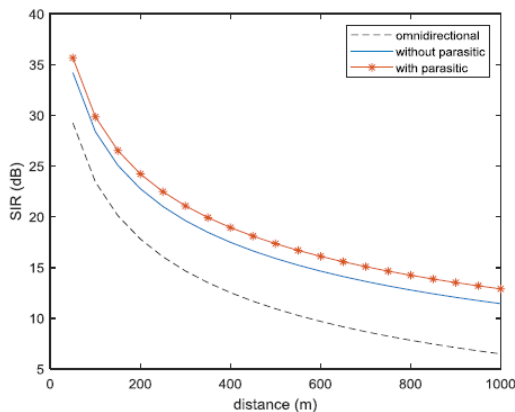


Fig.23. SIR and distance between cell site and user.

Conclusion

This article has proposed the mm wave switched beam antenna that operate at 28.5 GHz. Main beam directions are steered by shorted circuit at the corner of octagonal patch. Moreover, side lobe level can be reduced by using a parasitic ring. Shorting positions, outer and inner radius of parasitic are adjusted to obtain the lowest S_{11} at 28.5 GHz. There are 4 cases of switching which main beam directions are $119^\circ/299^\circ$, $154^\circ/334^\circ$, $27^\circ/207^\circ$ and $63^\circ/243^\circ$. The performance in term of SIR when utilizing omni-directional antenna, the proposed antenna with and without a parasitic ring are compared. The results confirm that the proposed antenna, the octagonal patch with a parasitic ring, can enhance the performance of the system.

Financial support from the Faculty of Engineering, Srinakharinwirot University, through the research grant No. 544/2562 is acknowledged.

Authors: Assist. Prof. Dr. Pichaya Chaipanya, E-mail: pichayac@g.swu.ac.th; Apirat Mana, E-mail: apirat932@gmail.com; Thanet Jiamdenngam, E-mail: thanetpn@gmail.com; Watcharapol Montree, E-mail: misterfrankz71@gmail.com. Department of Electrical Engineering, Srinakharinwirot University, Nakhon Nayok, Thailand.

REFERENCES

- [1] Denis A., Overview of ITU-T Activities on 5G/IMT-2020, *ITU Committed to Connecting the World*, (2020)
- [2] Gross Frank B., Smart Antenna for Wireless Communications with MATLAB, 1st ed., *McGraw-Hill*, (2005), ch 8.
- [3] Nakano H., Eto J., Okabe Y., Yamauchi J., Tilted- and Axial-Beam Formation by a Single-Arm Rectangular Spiral Antenna with Compact Dielectric Substrate and Conducting Plane, *IEEE Transactions on Antennas and Propagation*, 50 (2002), No. 1, 17-24
- [4] Mehta A., Mirshekar-Syahkal D., Pattern Steerable Square Loop Antenna, *IEEE Electronic Letters (IET)*, 43 (2007), No. 9, 491-493
- [5] Ngamjanyaporn P., Phongcharoenpanich C., Akkaraekthalin P., Krairiksh M., Signal-to-Interference Ratio Improvement by Using a Phased Array Antenna of Switched-Beam Elements, *IEEE Transactions on Antennas and Propagation*, 53 (2005), No. 5, 1819-1828
- [6] Uthansakul M., Chaipanya P., Uthansakul P., Performance Evaluation of a Low-Cost Switched-Beam Antenna for WLAN Users, *Microwave and optical technology letters*, 52 (2010), No. 9, 2069-2074
- [7] Chaipanya P., Uthansakul P., Wongsan R., Uthansakul M., Enhancement of WLAN Signal Strength using Switched-Beam Single Antenna, *APMC 2009*, (2009), 770-773
- [8] Yusnita R., Muhammad I.H., Design of 28/38 GHz Dual-Band Triangular-Shaped Slot Microstrip Antenna Array for 5G Applications, *International Conference on Telematics and Future Generation Networks (TAFGEN)*, (2018), 93-97
- [9] Hala M.M., Mohamed I.A., Abdelhamed A. Shaalan, Novel Dual-Band 28/38 GHz MIMO Antennas for 5G Mobile Applications, *Progress In Electromagnetics Research C*, 93 (2019), 103-117
- [10] Osama M.H, Mohamed M.M.A., Saleh A., Abdel-Razik S., Design of a 28/38 GHz Dual-Band Printed Slot Antenna for the Future 5G Mobile Communication Networks, *2015 IEEE International Symposium on Antennas and Propagation & USNC/URSI National Radio Science Meeting*, (2015), 1532-1533
- [11] Humberto A., Antonio de F., David P., Ivan C., Carlos C., A Multiband Antenna Design Comprising the Future 5G Mobile Technology, *Przeegląd Elektrotechniczny*, 2 (2019), nr 95, 108-111
- [12] Jing Z., Xiaohu G., Qiang L., Mohsen G., Yanxia Z., 5G Millimeter-Wave Antenna Array: Design and Challenges, *IEEE Wireless Communications*, 24 (2017), Issue. 2, 106 - 112
- [13] Balanis C.A., Antenna Theory: Analysis and Design, 4th ed., *J. Wiley & Sons*, (2016), ch 14
- [14] Mokal V., Gagare S.R., Labade R.P., Analysis of Micro strip patch Antenna Using Coaxial Feed and Micro Strip Line Feed for Wireless Application, *IOSR Journal of Electronics and Communication Engineering (IOSR-JECE)*, 7 (2017), Issue. 1, 36-41
- [15] Khan F., LTE for 4G Mobile Broadband Air Interface Technologies and Performance, *Cambridge University Press*, (2009), ch 16
- [16] Goldsmith A., Wireless Communications, *Cambridge University Press*, (2007), ch 4